This project has received funding from the European Union's Horizon 2020 research and innovation programme under grant agreement No 101036458.

Module for Risk Assessment from Energy Systems

D4.4

Pol Paradell
Nuria Cantó
Jose Luis Domínguez
Albert Gili
IREC

LOCALISED

Disclaimer

This report was written as part of the LOCALISED project under EC grant agreement 101036458. The information, documentation and figures available in this deliverable were written by the LOCALISED project consortium and do not necessarily reflect the views of the European Commission. The European Commission is not liable for any use that may be made of the information contained herein.

Statement of originality

This deliverable contains original unpublished work except where clearly indicated otherwise. Acknowledgement of previously published material and of the work of others has been made through appropriate citation, quotation or both.

How to quote this document

Paradell, P. et al, (2025), Module for Risk Assessment from energy systems (LOCALISED Deliverable 4.4)

General information about this Document

Project acronym	LOCALISED
Project full title	Localised decarbonisation pathways for citizens, local administrations and businesses to inform for mitigation and adaptation action
Grant Agreement no	101036458
Deliverable number	D4.4
Deliverable title	Module for Risk Assessment from Energy Systems
Deliverable nature	Report
Dissemination level	Public
Work package and Task	WP4; Task 3
Contractual delivery date	March 2025
Actual delivery date	March 2025
Authors	Pol Paradell, Nuria Cantó, Jose Luis Domínguez and Albert Gili (IREC)
Reviewers	Komal Vendidandi (PIK), Christiane Walter (PIK), Soheil Shayegh (CMCC)

Revision History

Version	Date	Name
1st Version – Definition ToC	11/12/2024	Albert Gili (IREC)
2nd Creation of content	20/03/2025	Pol Paradell, Jose Luis Dominguez and Nuria Cantó (IREC)
3rd Finalize content	21/03/2025	Pol Paradell, Jose Luis Dominguez and Nuria Cantó (IREC)
4th Address to review comments	28/03/2025	Pol Paradell (IREC)
5th final version	31/03/2025	Pol Paradell, Nuria Cantó (IREC)
6th minor modifications	01/04/2025	Pol Paradell (IREC)
Final revision	14/11/2025	Pol Paradell, Jose Luis Dominguez and Nuria Cantó (IREC)

Table of Contents

1 List of Figures

2 List of Tables

3 List of Abbreviations

A_A	Affected Area
A_B	Buffered Area or area of flooding influence
AAR	Affected Area Rate
ASAI	Average Service Availability Index
AWD	Average of Water Depth
BAS	BAseline Scenario considered in flood models
BAU	Business As Usual scenario considered in flood models
CAIDI	Customer Average Interruption Duration Index [min]
CD / CDs	Electrical Center of Distribution
CRS	Coordinate Reference System
DSO	Distribution System Operators
FEMA	Federal Emergency Management Agency of United States
FP	Failure Probability
GEN	Generator
GIS	Geographical Information System
HV	High Voltage Substation
LV	Low Voltage
MV	Medium Voltage Substation
REBT	Low Voltage Electrical Regulations (Reglamento Eléctrico de Baja Tensión)
RESCCUE	RESilience to cope with Climate Change in Urban arEas – a multisectorial approach focusing on water. H2020 project.
RT	Repair Time
SAIDI	System Average Interruption Duration Index [min]

SAIFI	System Average Interruption Frequency Index
SUD	Sustainable Urban Drainage system set of measures applied to flood models
TWE	Time Without Energy
USM	Urban Storm-water Model

1 Executive Summary

The document is addressed to the project partners and energy sector researchers to provide the energy sector's risk assessment results. The document underscores the urgent need to address the impacts of climate change on the energy sector, with a particular focus on the risks of fires and heat waves across various regions. It highlights how these events can severely impact energy systems and infrastructure, necessitating the immediate implementation of resilient and adaptive strategies to mitigate these risks.

Module 4.4 is a comprehensive tool for risk assessment in the energy sector designed to evaluate and address these challenges. It utilises data generated from WP2 and WP3 on climate impact metrics using the RCP pathways. This module rigorously evaluates the effects of climate change on energy systems at a NUTS3 resolution.
The module provides a robust framework for quantifying impacts on the electrical sector, considering factors such as fire risks and heat waves. It offers methodologies for correcting impact analysis and addressing electrical model considerations. It serves as a valuable resource for understanding regional climate impacts and supporting decision-making processes in the energy sector.

In conclusion, the document underscores the practicality and necessity of addressing climate-related risks in the energy sector. It presents Module 4.4 as a user-friendly and effective tool for assessing and managing these risks and strongly encourages its immediate adoption for effective risk management.

2 Introduction

Due to climate change, extreme weather events are prone to occur. In this regard, critical electrical infrastructures must be secure and resilient to the impact of extreme events. Due to the high-density population characteristic, regional and urban areas are the most sensitive and critical zones if hit by an unexpected climate extreme event. This reason is why regional resilience is a key topic being investigated worldwide. In this deliverable, the development of a risk assessment module for the electrical sector is explained, which is oriented to help decision-makers in planning, providing unitary and global views of the electric assets of a network and their interrelation in a failure case by assessing the risk, the cost and the electric network reliability indices. Additionally, this module can be easily applied to different scenarios, showing the impact of the various energy future scenarios and risks.

Up to now, some related works have tried to address these problems. The references [7–9] seek to assess the grid's resilience through energy economic losses in power interruptions by modelling the behaviour of the grid at macro and micro scales and allowing the DSOs to make decisions in energy planning and operation. Researchers in [10,11] focused only on flooding risk assessment through spatial network models and HAZUS methodology [12]. However, the most complete and related risk study was carried out in [13], using fragility curves in GIS-based methods to assess the risk posed by seismic events on the electrical and gas networks. Also, in [14,15], a methodology is developed to estimate economic losses provoked by electrical assets in flooding events from which some equations of the methods used on the tool are part.

3 Resiliency and risks for the energy sector

In resilience, the electric power system is considered a critical infrastructure. Due to the latter, the power system has already been designed to be reliable and withstand specific unexpected outages by following the criterion of *N-k*. In the energy system, the (n-k) criterion, commonly referred to as (n-k) safety, explains that even if a power grid component fails, the supply is still ensured by redundancies, preventing a system failure. This criterion is a cornerstone of most European electrical network architecture and plays a significant role in the country's high degree of network security. Existing backup plans stop the supply from cutting off or the fault from getting worse if a component, like an electrical circuit, fails.. However, it is recognised that the system should be designed for an even higher number of component losses due to the effects of climate change, which would challenge the system to withstand high-impact and Low Probability (HILP) events due to extreme weather scenarios. Such scenarios may lead to cascade outages or parallel failures, implying a loss of resilience. The power grid resilience can be understood as the capacity of the network to absorb, adapt and recover from extreme events Figure 1.

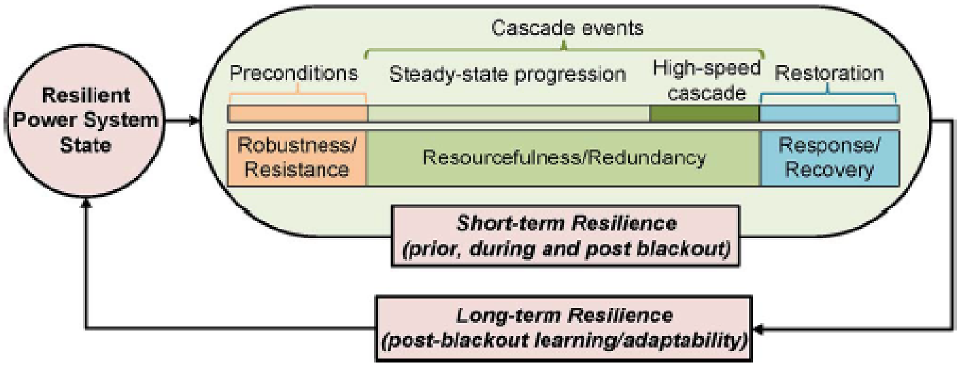

Figure 1. Short and long-term resilience of power system (Panteli & Mancarella, 2015)

From a climate-based perspective, the distribution power supply network is sensitive to impacts from high and low temperatures, rainfalls, and floods. In the UK in 2015, for example, the power supply network failed in the cities of Rochdale and Lancaster due to separate flood incidents. In the United States alone, the number of weather-related power outages between 2003 and 2012 was estimated to account for costs higher than 300 billion US dollars (Gholami et al., 2016).

Furthermore, it is essential to assess those areas directly affected by extreme events and those areas that, although not located in the damaged zone, might indirectly be affected for various reasons. Such reasons could be the loss of generators or loads in the area directly affected by the event, causing instabilities in the grid (Figure 2). As observed, if preventive actions are considered, the system's resilience can be recovered in a much shorter period.

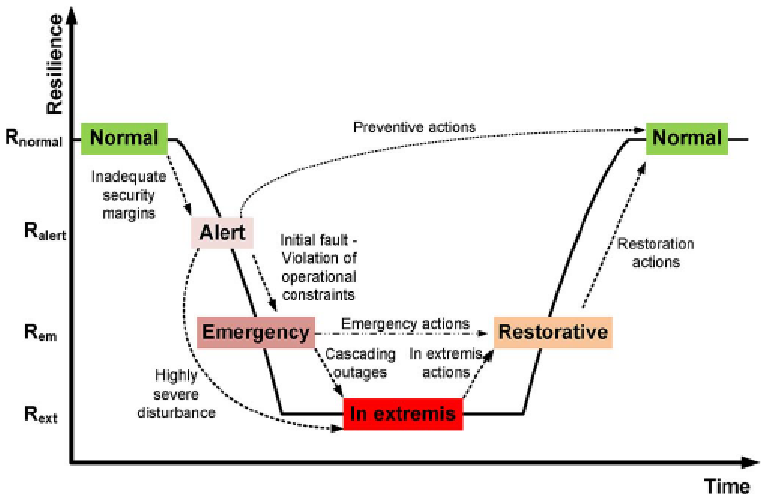

Figure 2. Conceptual resilience curve (Panteli & Mancarella, 2015)

Quantifying electric power grid resilience to cope with climate change in urban areas is an essential current challenge due to recent notable disasters in some developed countries and our society's increasing dependence on electricity. However, obtaining resilience metrics in power grids is a complex task that involves taking into consideration several aspects, such as the effect and influence of humans in the power system's performance, the interdependencies between loads and generating units or the shift towards a more distributed customer system where local energy storage systems and smart-grid technologies play a significantly important role, among others. As stated by Gholami et. al. (2016), current centralised power systems, i.e. energy flow going downstream, from generation plants to loads, pose a limit to the recovery of critical loads as the restoration process is also top-bottom. The highlighted weaknesses of centralised power systems have illustrated the opportunities for Distributed Energy Resources (DER), distributed energy storage (batteries, electricity, vehicles, …) and microgrids to enhance resilience.

By observing in detail the components within the distribution power network, fragility curves could be used to determine the probability of failure depending on different climate variables, such as wind speed, temperature, and water coverage. For instance, the transformer substations scattered throughout a city are responsible for decreasing domestic and commercial voltages. The probability of failure of these electrical assets could serve as a means of finding out the vulnerable zones within the electrical system. For instance, from a flooding perspective, the proposal would be to map the substations' locations and overlap them with flood depth maps with associated damage depth curves. This way, it would be possible to establish the likelihood of failure of these substations throughout the city, as Panteli and Mancarella (2015) stated.

Additionally, risk is understood as the possibility of something bad happening. Usually, risk can be defined as the combination of the probability of an event and its consequence. In general, this can be explained as:

Risk = Likelihood × Impact.

Where **likelihood** refers to the probability of occurrence of the event, and i**mpact** refers to the quantification of the resulting occurrence.

In other words, considering the energy sector, it could lead to the following questions, how much energy is not supplied? How much does it cost? How many components are broken? What is the criticality of this happening?

Power systems have various potential risks that depend on the components, location, and event. Wind may affect Overhead lines but not underground systems, or the impact of flooding is more critical to buried systems than those at certain heights from the ground. Also, there are risks related to artificial impacts (so, how reachable is the component?), or Cyber-attacks may impact "connected" systems.

Certain features within the power distribution chain are vulnerable to failure. An example is the transformer substations scattered throughout a city that are responsible for decreasing voltages for domestic and commercial use. In order to analyze the impact of climate hazards on the electrical network of an urban town, several approaches can be carried out. On the one hand, with the aim of having an insight into the severity of damage from a quantitative point of view, several indicators can be calculated to quantify the performance of the power system under abnormal circumstances produced by some extreme event. These resilience metrics are explained in detail in the following section.

On the other hand, a statistical analysis can be performed to identify vulnerabilities in the electrical network. This type of study is based on considering fragility curves, which indicate the probability of a particular component reaching a certain damage state. Thereby, the probability of occurrence of a certain component failure can be calculated by considering the probability distributions of the different climate variables. For instance, from a flooding perspective, the proposal here would be to map the locations of substations via the analysis of flood depth maps with associated damage depth curves (or fragility curves which represent the probability of failure occurrence (as shown in the following figure 3) to establish the risk/likelihood of failure of these substations throughout the city.

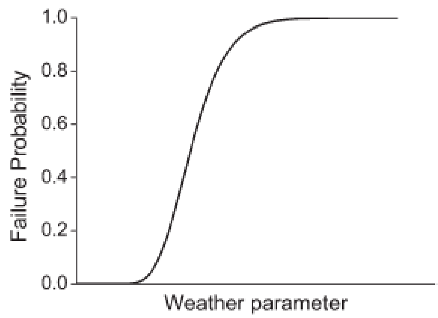

Figure 3. Determining components' failure probability using fragility curves (Mathaios Pantelia, Pierlugi Mancarella Volume 127, October 2015, Pages 259-270)

To evaluate the impact of weather on power systems' resilience theoretically, there is a need to model several components, including the stochastic nature of weather and the reliability of the components. For this as highlighted by Panteli & Mancarella (2015), there are diverse modelling requirements to consider as *simulation procedure* (for example, Analytic -e.g. using Markov Chains or only equations- useful for small-scale systems or Monte-Carlo simulations, to consider stochasticity of weather, failure and restoration rates, etc.), *independent and common cause failures, impact of human response during weather emergencies, restoration times, weather regions, among others.*

3.1 Quantifying impacts on the electrical sector

To quantitatively represent the power grid's performance during natural disasters or other extreme events, Kwasinski (2016) proposed the following metric for resilience applied to the energy supply sector based on the definition of resilience currently adopted by several agencies and national laboratories around the world, such as for example Department of Energy (DOE) in U.S. or U.K. Cabinet office (i.e., "the ability to prepare for and adapt to changing conditions and withstand and recover rapidly from disruptions").

$$R_B = \frac{\sum_{i=1}^{N} T_{U,i}}{NT} = \frac{\sum_{i=1}^{N} T_{U,i}}{\sum_{i=1}^{N} (T_{U,i} + T_{D,i})} \quad (1)$$

where R_B is the base resilience, N is the number of loads in the studied system, T is the period of time under consideration, $T_{U,i}$ is part of T when a load i is able to receive electric power and $T_{D,i}$ is the remaining portion of time T when load i may not be able to receive electric power (downtime).

According to the literature (Willis, et al. (2015)), there are multiple ways to assess how resilience is managed and measured in energy systems. System Operators and Utilities have developed several performance metrics concerning different critical aspects such as energy delivery, reliability, power quality and sustainability to measure system performance. According to Kwasinski (2016), power outages are considered the primary performance indicator for evaluating the impacts of extreme events on the power grid. The amount of interruptions determines supply continuity; therefore, System Operators and Utilities aim to minimise interruptions to maximise power availability. Since affections to the power system are very particular for each case, it is hard to define reference values.

As can be seen in Figure 4, the period of time ranging from one extreme event to the next can be divided into different phases:

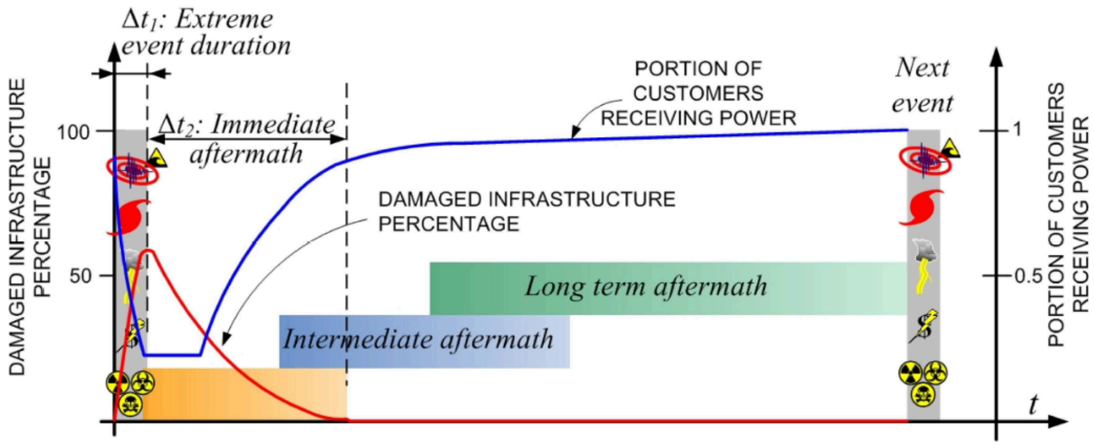

Figure 4. Representation of the phases of an extreme event and their aftermaths (Kwasinski, 2016)

Based on reliability theory and *IEEE* Standards, electric utilities consider several supply continuity indicators as resilience metrics of the power grid. Additionally, power quality is determined by both the voltage waveform, which is the quality of the product delivered, and the supply continuity, which determines the availability of the product.

Regarding supply continuity, the *IEEE Guide for Electric Power Distribution Reliability Indices* includes sustained interruption metrics that can be classified as:

a) **Customer-oriented indices**

- **System Average Interruption Frequency Index (SAIFI)** indicates the average number of interruptions by the electrical consumer, the customer that uses the electricity, in a defined period.

$$SAIFI = \frac{\sum Total\ number\ of\ customers\ interrupted}{Total\ number\ of\ customers\ served} \quad (\ SEQ\ Ecuación \setminus *\ \ ARABIC\ 2)$$

- **System Average Interruption Duration Index (SAIDI)** indicates the average outage duration for each customer served. It is usually measured in minutes or hours.

$$SAIDI = \frac{\sum Customer\ interruption\ durations}{Total\ number\ of\ customers\ served} \quad (3)$$

- **Customer Average Interruption Frequency Index (CAIFI):** this index indicates the average frequency of interruptions by customers interrupted.

$$CAIFI = \frac{\sum Total\ number\ of\ customers\ interruptions}{Total\ number\ of\ customers\ interrupted} \quad (4)$$

- **Customer Average Interruption Duration Index (CAIDI)** indicates the average outage duration by a customer interrupted.

$$CAIDI = \frac{\sum Customers\ interruption\ duration}{Total\ number\ of\ customers\ interrupted} = \frac{SAIDI}{SAIFI} \quad (5)$$

- **Average Service Availability Index (ASAI):** this index indicates the fraction of time that service was available to a customer during the defined reporting period. It is normally expressed as a percentage.

$$ASAI = \frac{Customer\ time\ service\ availability}{Customer\ time\ service\ demands} = 1 - \frac{SAIDI}{8760} \quad (6)$$

b) Load oriented indices

- **The average System Interruption Frequency Index (ASIFI)** indicates the equivalent number of interruptions out of the total served load.

$$ASIFI = \frac{\sum Total\ connected\ kVA\ of\ load\ interrupted}{Total\ connected\ kVA\ served} \quad (7)$$

- **The average System Interruption Duration Index (ASIDI)** indicates the equivalent duration of interruptions out of the total served load.

$$ASIDI = \frac{\sum Connected\ kVA\ duration\ of\ load\ interrupted}{Total\ connected\ kVA\ served} \quad (8)$$

c) Generation/Transmission system-oriented indices

Power Indices:

- **Loss Of Load Expectation (LOLE):** this index indicates the expected number of days per year during which the system is not able to cover the daily peak demand.

- **Loss Of Load Probability (LOLP):** this index indicates the annual probability for which the system is not able to cover the daily peak demand.

Energy Indices:

- **Loss Of Energy Expectation (LOEE)**: this index indicates the expected energy for which the system will fail to serve during a period of time, usually considered one year.
- **Energy Not Supplied (ENS)**: this index indicates the energy the system has not supplied during a considered period.

4 Methodology applied for risk assessment

The methodology applied in this report is based on the one proposed in [16], which was developed within the RESCCUE project, but some improvements on specific analyses and functions have been performed. This methodology has been implemented as an analysis tool based on QGIS and Python, easing its usage and application in a variety of cases.

The methodology can perform analyses for electrical assets based on risk assessment, failure estimation, cost assessment, and the calculation of electrical reliability indices. Additionally, electrical grid estimation, European-wide, has been included using the EU-PyPSA tool.

Finally, the capability of analyzing the radial relationship established through the electrical network between locations has been added. The subsequent cumulative failure probability calculation for each of the last points of the grid is known as the cascading effect on power systems.

A graphical explanation of the new methodology presented and used in this paper is given in Figure 5.

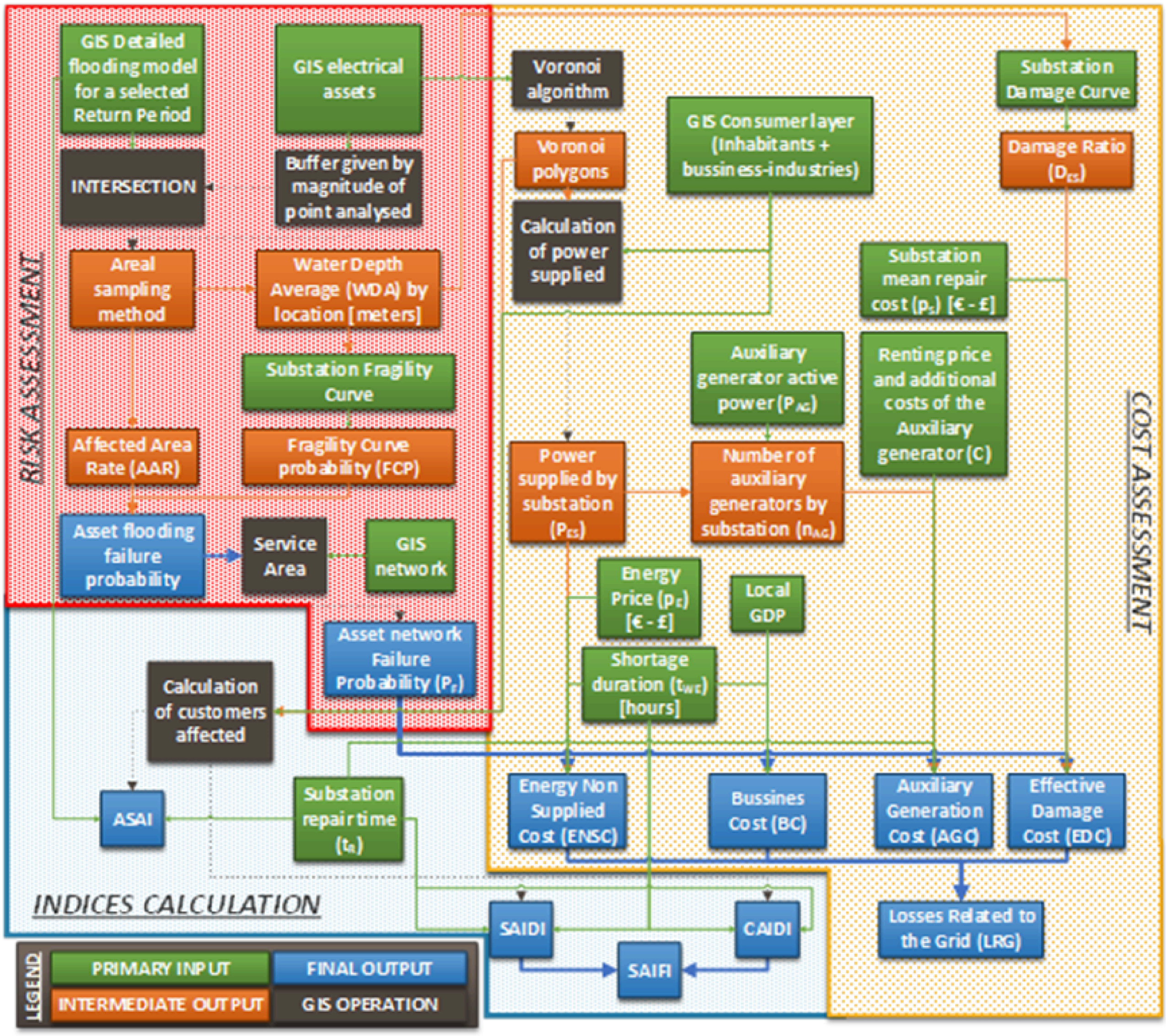

Figure 5. Graphical explanation of the methodology of the process developed in QGIS where the data is processed and manipulated by different GIS algorithms from several data inputs.

4.1 Impact analysis correction

The sampling method developed consists of the aerial calculation of the average risk contained within the affected influence area (i.e., extreme weather effect). In this way, there is no place for errors provoked by the uncertainty of the sampling points location since the proportions of impacted parts are precisely measured in the areas of influence generated for each location (Figure 6). this image is a sample of a zoom showing only 3 electrical assets, the red dots (in this case, electrical distribution centres). The risk zone is calculated in blue, and the circles around assets are the influence areas (in green, in case of no affectations and in red, the affected).

Figure 6. The sampling method based on measuring the affected and non-affected areas and the water depth data contained.

This modification changes the way how some of the base parameters are calculated. The Affected Area Rate (AAR) is calculated by taking the area affected (A_A) of each location and dividing it by the total area sampled (area of influence generated by a buffer algorithm (A_B)) (Equation(9) below). The affected area is calculated by intersecting the buffered area with the impact layers and extracting the polygons within the buffered area, which contain information on the estimated critical parameters (i.e. wind speed, water depth, etc.).

$$AAR = \frac{A_A}{A_B} \quad (9)$$

For calculating the Average Water Depth (AWD), the weight of each polygon is computed in reference to the affected area. This ratio is used to weigh the influence of the polygon water depth over the total area affected (Equation$AWD = \sum_{i=1}^{n} WD_i \frac{A_{local_i}}{A_A}$ (10) and keep the weighted average of water depth. To prevent insignificant values from being obtained, the AWD was filtered to eliminate all values below 0.1 m, on the assumption that all electrical assets would count with a minimum elevation of that level.

$$AWD = \sum_{i=1}^{n} WD_i \frac{A_{local_i}}{A_A} \quad (10)$$

The value obtained after calculating the AWD of each polygon is introduced in the fragility curve shown in Figure 7 to calculate the potential failure probability of every single electrical asset affected by extreme events, and after that, calculate the damage and repair time curves.

The fragility curve provides the probability of failure of the assets analysed in this analysis adapted from FEMA [12] (created for assessing electrical substations of all categories). From our perspective, this should be extended and adapted for each type of substation because each one has its own construction standards and typical weather-based measures already applied, and the fragility curve quality significantly affects the assessment performance [16]. A sensitivity analysis may be applied to avoid such uncertainty if real data is not in use.

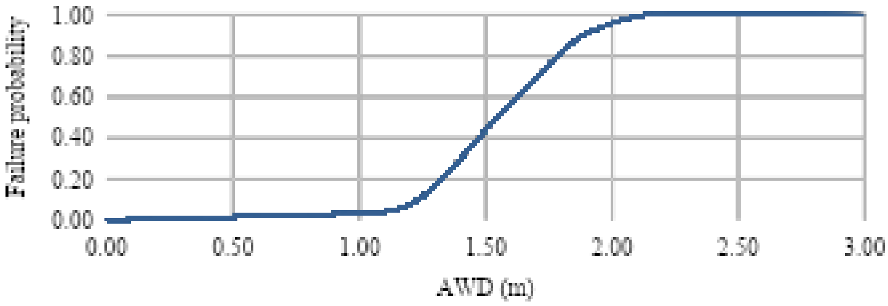

Figure 7. The fragility curve employed in the tool (Adapted from FEMA [12])

4.2 Electrical model consideration

When only distribution centres are studied, including the other network assets to analyse the flooding risk is unnecessary since these represent the last link in the distribution network. It must be noted that the network feature refers to the electrical connection among different nodes and grid elements. However, when including higher-grade substations in the analysis, the interactions between the network nodes must be defined. The grid topology defines these interactions. Commonly, the topology of the grid mixes radial and mesh connections. Still, in the methodology presented here, only the radial topology has been implemented, which is the most common electric connection method at the LV distribution grid. Such interconnection is relevant and considered as input on the methodology presented to achieve close-to-reality results.

Table 1 shows how the connections between assets of different grades are created, joining each grade with its consecutive.

Thus, adding a new grade substation layer will mean an additional process, creating a new set of lines defining those connections. After creating all the lines, these will be merged into one single network. Additionally, a field with the direction of the flow must be created (always "forward" in a radial network since the flux cannot go back) and used by the algorithm responsible for finding the service area of the affected locations.

ASSET GRADE	**ASSET ID**	**CONNECTION**			
	Name	**Supplier 1**	**Supplier 2**	**Supplier n**	**Direction**
G1	GEN	-	-	-	Forward
G2	HV	GEN 1	GEN 2	GEN n	Forward
G3	MV	HV 1	GEN 1	-	Forward
G4	CD	MV 1	HV 1	-	Forward
		1 process	*2 processes Merged*	*n processes*	

Table 1. Electrical assets layer mandatory columns and example of filling.

Once the network is created, the indirectly affected intermediate and endpoints can be traced by following the paths created from the directly affected locations. After that, all the locations directly and indirectly affected are identified and gathered within a single layer, with the cumulative probability of failure calculated in cascade, as shown in Equation (11). This equation represents a sum of probabilities that are not linked, meaning there is no relation or interference between them.

$$FPfinal = 1 - (1 - G1) * (1 - G2) * (1 - G3) \qquad (11)$$

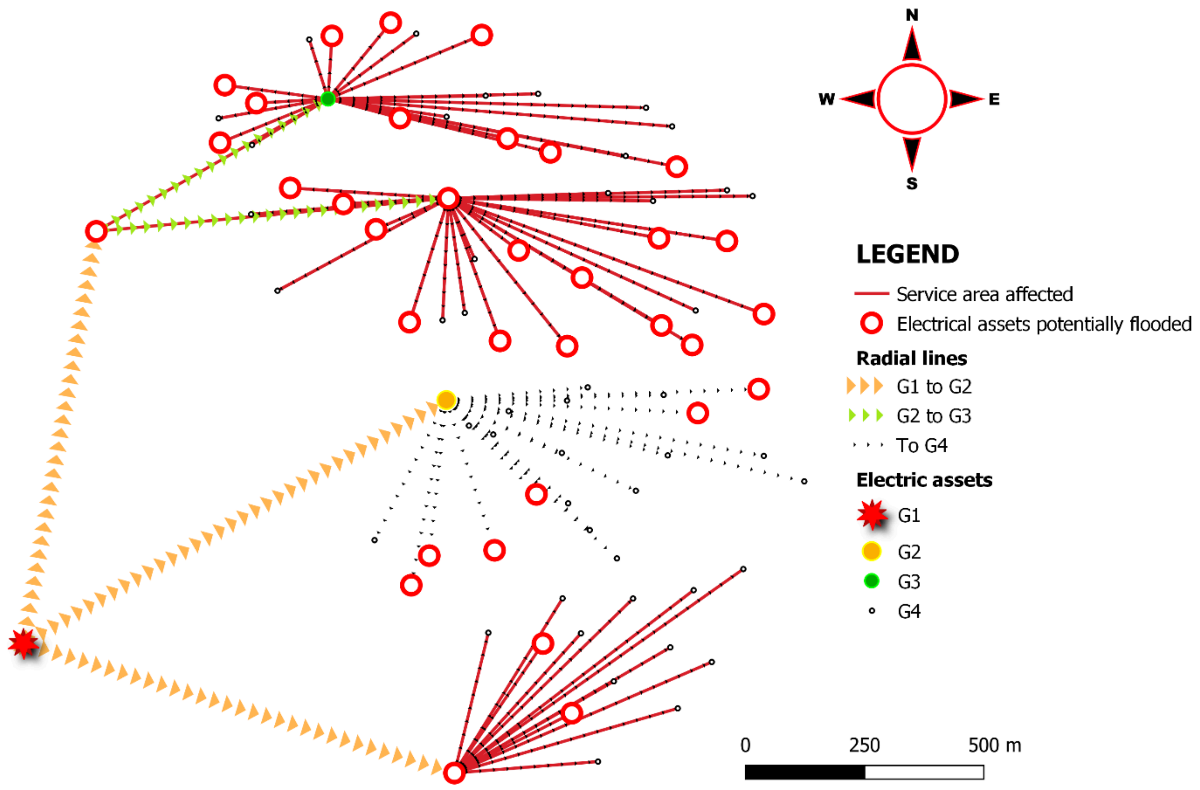

Figure 8. Example of radial network for application within the model.

After calculating the cumulative FP values for all the locations, the cost assessment will be performed in the same way as proposed in [16].

	Electrical asset layer		Network layer	Flooding layer	Consumer layers	
Description	*A point layer with the geolocation of the assets*		*A polyline layer is derived from the electrical asset layer.*	*A polygon layer with flooding*	*Two-point layers estimating the human and industrial/business consumers of the study area*	
Fields	Radius (m)	Voltage (kV)	Flow Direction	Water Depth (m)	Consumption (kWh)	Weight

Purpose	Estimation of the surrounding influence area	Calculation of the damage cost of the substation.	Calculation of service area affected	To calculate the AWD, AAR, FP, and Damage.	To estimate the power losses	Represents the number of consumers estimated at each point

Table 2. gathers the four main inputs needed to complete the analysis and the fields to include in each layer from where the tool will take the data to accomplish all the operations.

5 Module 4.4

Module 4.4 is designed to perform a risk assessment on the energy sector using the information generated on the Localized project, principally from WP3 and WP2, and electrical assets provided by Pypsa-eur. The module's principal objective is to analyse the effects of different hazards detected in the energy sector in terms of probability.

The module uses information from different sources: The geographical information at the NUTS3 level to have the borders of each region. The electrical grid needs to have the location of the other assets on it. Finally, uses data on risk probability for different hazards, provided as results from other modules of the project, such as ETHOS.MIDAS. With this information, the module calculates the impacts on the energy sector; these impacts can vary and must be analysed individually. The module calculates the risk of fire and heatwaves. These risks were studied because the values recorded for these hazards were more significant, given the information needed for this specific risk assessment.

This hazard could impact the entire system in a fire by affecting energy generation or electricity transmission. The fire could impact the electricity transport system more because it goes across all the regions. The module evaluates all the electrical lines and assigns the maximum risk to all areas within each line.

The risk of heat waves is another hazard that directly impacts energy systems, as it stresses the transport system. As temperatures decrease, the capacity of the lines increases. Indirectly, it increases energy demand, putting pressure on the energy generation and transport systems. For these reasons, the lines regarding this risk will be analysed and evaluated for their impact on the energy system.

5.1 Module 4.4 details

Module 4.4 performs various steps to assess the impacts on the energy sector. Figure 9 shows a flow diagram of the steps performed by the module. The first task is to download the borders at the NUTS3 level, as it is important to have the maximum resolution. It is saved in a geopandas reformat to use the borders of each region later to locate and relate between the electrical assets and the risks.

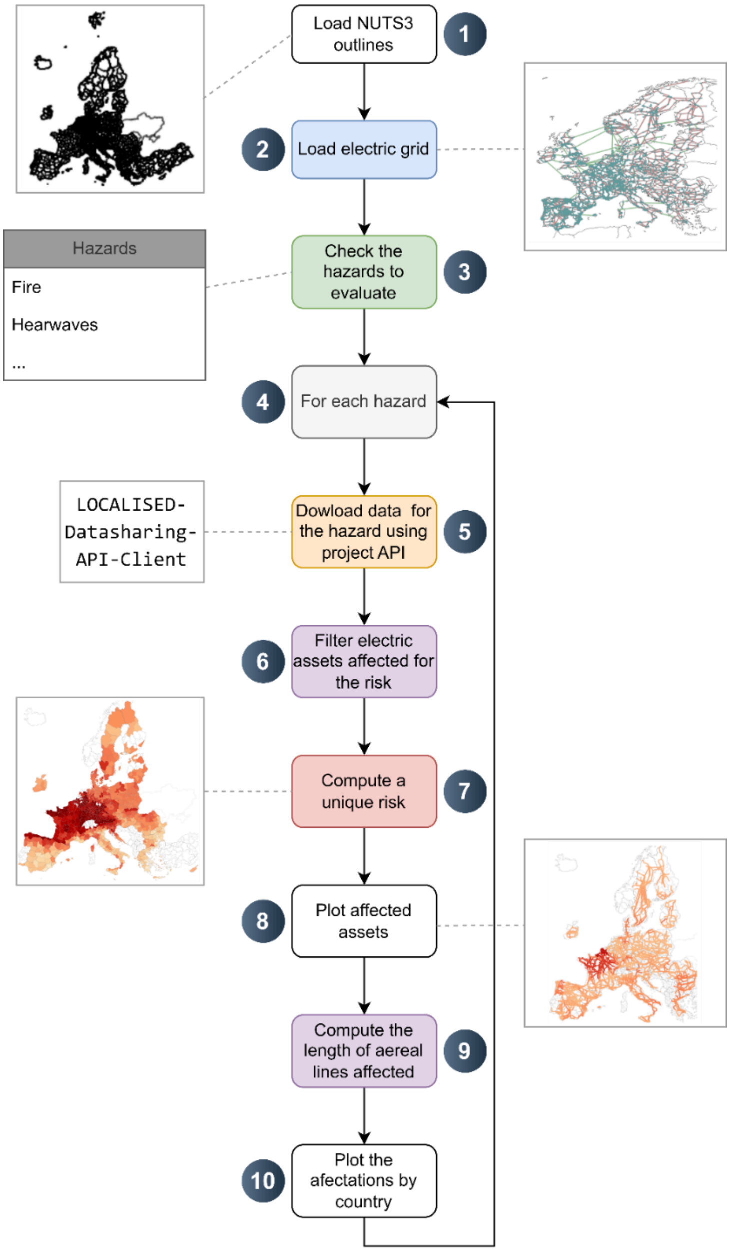

Figure 9. Module 4.4 flow diagram

The next step is to gather the electrical system. It downloads the information about the electrical system provided by Pypsa-eur. This source is a public repository for computing the electrical system, providing information on all available installations and electrical assets. The electrical grid is shown in Figure 10, all this information is essential for the module, as these assets are the ones that will be evaluated in terms of risk.

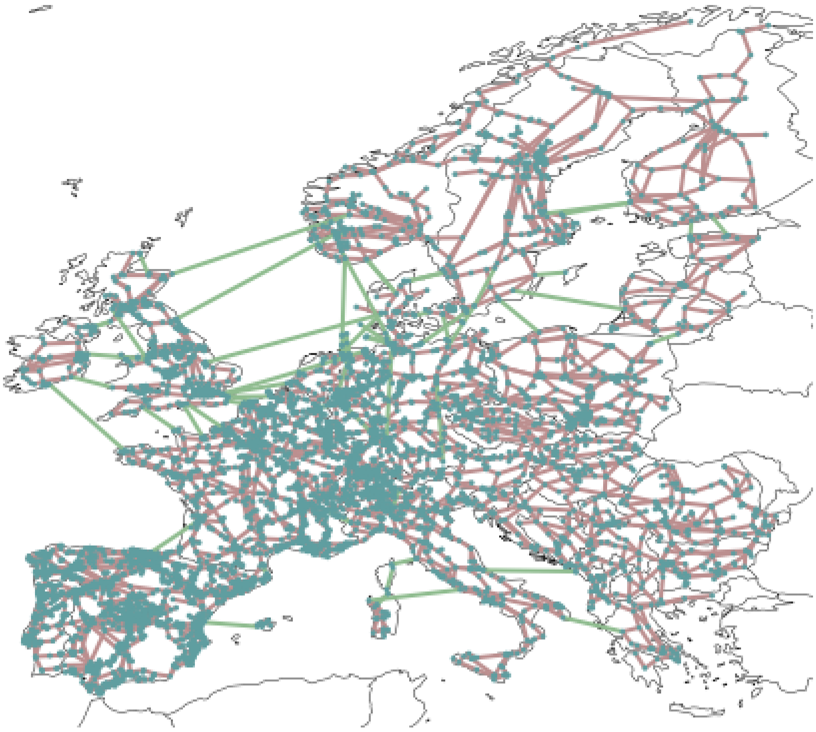

Figure 10. Electrical system from Pypsa-eur.

One of the most vulnerable assets in the energy system is the electrical aerial lines. The module utilises the electrical lines to calculate the affectations on the energy system, as these lines provide energy to all regions. Figure 11 shows the number of kilometres of electrical lines per country the module uses.

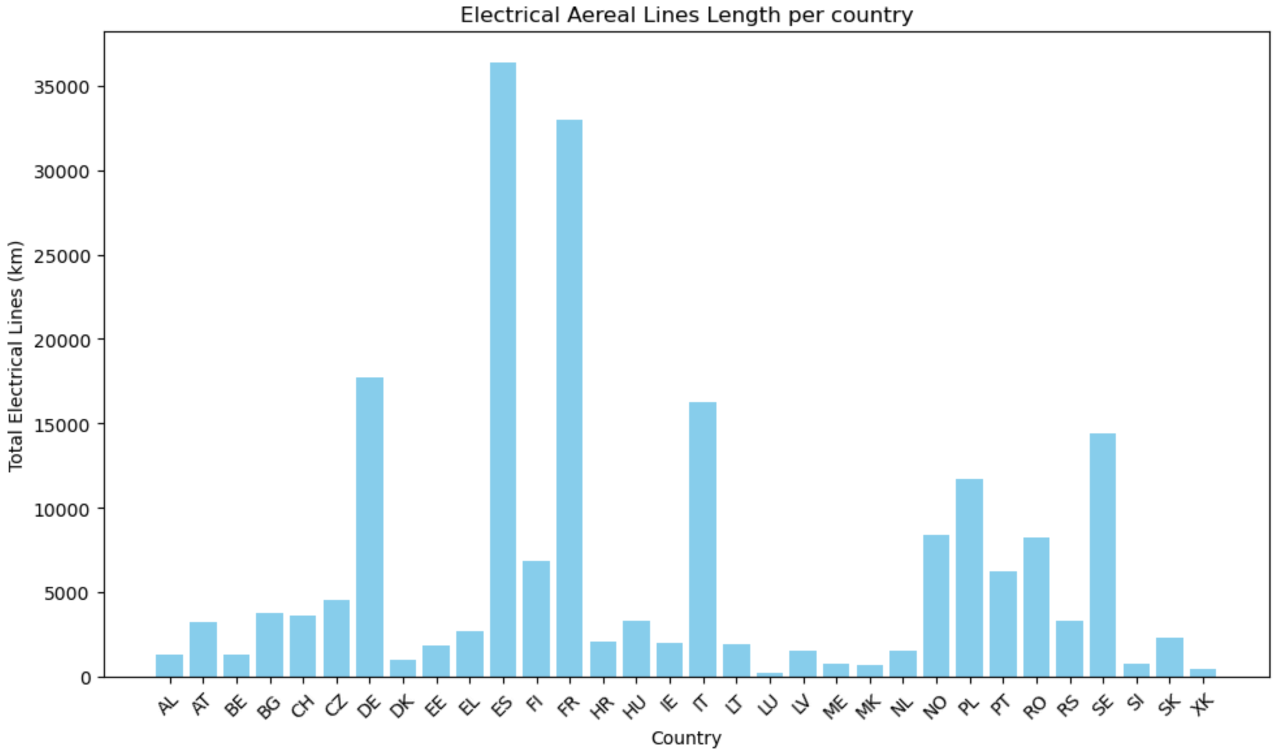

Figure 11. Aerial electrical lines per country.

The third step is to verify the available variables that can be used to calculate the risks associated with the electrical system. Based on previous experience with electrical systems, the variables are classified into different hazards that could impact the energy system. Once all the variables related to each hazard are identified, the module initiates a parallel evaluation of each risk, which is the fourth step.

In the fifth step, the chosen variables from the step tree are downloaded and structured in the same format. Then, in the sixth step, the module assigns risk to the lines based on their location. Additionally, if a line spans multiple regions, it takes on the highest risk in those regions.

In the seventh step, the different variables are combined to create a unique risk value. The approach used for this unique risk combines probabilities and assigns a weight to each risk to emphasise the most relevant risks. The weight of each risk is determined by the expert's experience. Then, in the last three steps, different graphics with the affected assets are created, and the percentage of length affected per country and NUTS3 region is computed.

6 Climate impacts per region

This section explains the climate impacts that have been evaluated and could affect the energy system. The data obtained from WP2 and WP3 classifies the information into different Representative Concentration Pathways (RCPs). The module utilises these various scenarios to assess the risks.

6.1 Fire risk

Evaluating the risk with the existent variables of the project has been used the following variables:

- Change in frequency of high fire risk: maximum and mean.
- Change in frequency of moderate fire risk: maximum and mean.
- Change in frequency of very high fire risk: maximum and mean.
- Change in intensity of high fire risk: maximum and mean.
- Change in intensity of moderate fire risk: maximum and mean.
- Change in intensity of very high fire risk: maximum and mean.
- Historical probability of high fire risk: maximum and mean.
- Historical probability of moderate fire risk: maximum and mean.
- Historical probability of very high fire risk: maximum and mean.
- The time frame of high fire risk: maximum and mean.
- The time frame of moderate fire risk: maximum and mean.
- The time frame of very high fire risk: maximum and mean.

All the previous variables are evaluated to be included in a unique risk assessment using the NUTS3 resolution. Figure 12, Figure 13 and Figure 14 show the cumulative fire risk on the different pathways. Thus, Table 3, Table 4 and Table 5 show the top 20 NUTS3 regions with high fire risk, where it can be observed that on RCP2.6, the risk is moderate, but on RCP4.5, the risk increases, especially in France. On RCP8.5, there is a high risk in most countries. The column NUTS_ID is the identification on NUTS3, NAME_Latin is the region's name using the original naming, the CNTR_CODE is the country's designation, and the Fire risk is the normalised value of fire risk calculated.

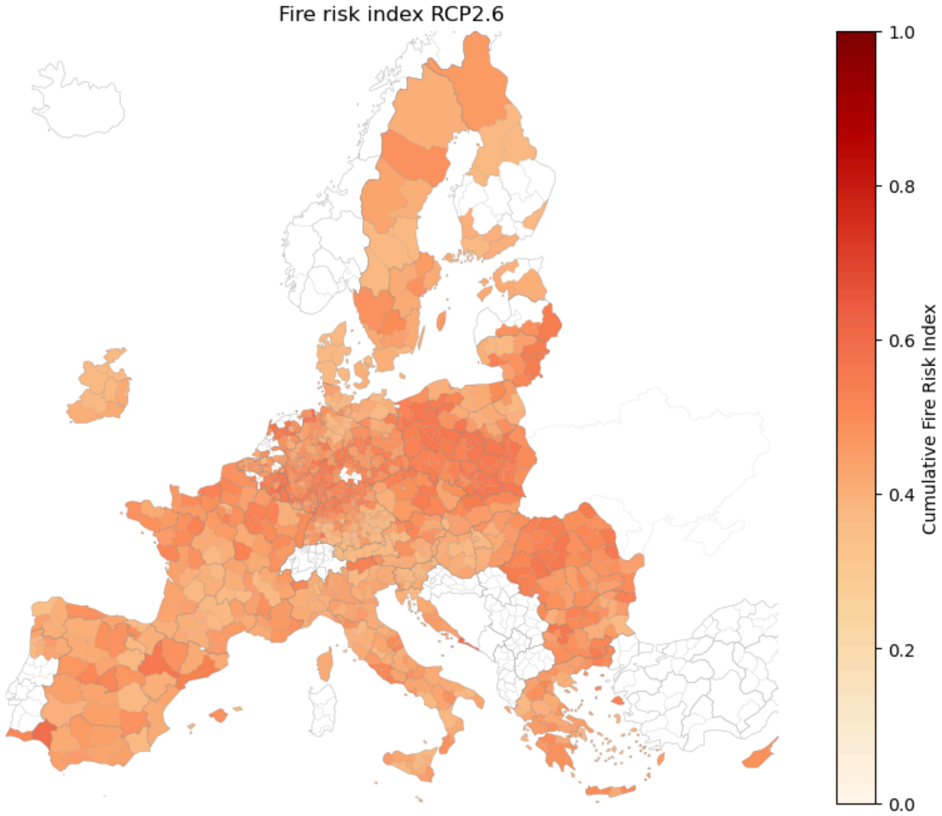

Figure 12. Unique fire risk RCP2.6.

Table 3 shows that the regions with high risk are heterogeneous around countries, but there is a marked difference in the other scenarios. In the RCP 4.5 scenario, Table 4, France is the most affected by the fire risk. On the RCP8.5, Table 5, the high risk is concentrated principally in central European countries.

NUTS_ID	**NAME_LATN**	**CNTR_CODE**	**Fire risk**
DE94A	Friesland (DE)	DE	0.6233
HR037	Dubrovačko-neretvanska županija	HR	0.5967
ES615	Huelva	ES	0.5833
BE342	Arr. Bastogne	BE	0.5833
DEB3E	Germersheim	DE	0.5833
PL418	Poznański	PL	0.5600
PL427	Szczecinecko-pyrzycki	PL	0.5600
NL126	Zuidoost-Friesland	NL	0.5600
PL414	Koniński	PL	0.5600
RO423	Hunedoara	RO	0.5600
DE718	Hochtaunuskreis	DE	0.5600
PL618	Świecki	PL	0.5600
DE719	Main-Kinzig-Kreis	DE	0.5600

PL619	Włocławski	PL	0.5600
PL22B	Sosnowiecki	PL	0.5600
PL712	Łódzki	PL	0.5600
PL713	Piotrkowski	PL	0.5600
PL715	Skierniewicki	PL	0.5600
PL721	Kielecki	PL	0.5600
DE137	Tuttlingen	DE	0.5600

Table 3. Top 20 high fire risk RCP2.6 by NUTS3.

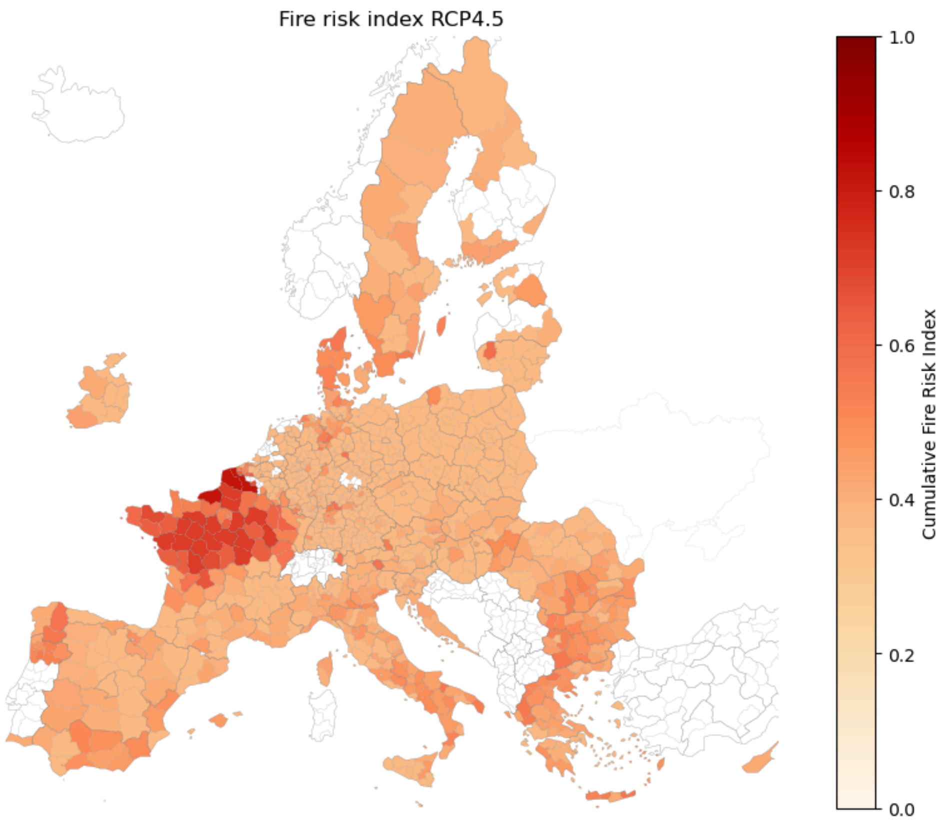

Figure 13. Unique fire risk RCP4.5.

NUTS_ID	NAME_LATN	CNTR_CODE	Fire risk
FRE12	Pas-de-Calais	FR	0.8200
FRE11	Nord	FR	0.8200
FRD22	Seine-Maritime	FR	0.8200
FRD13	Orne	FR	0.7200
FRF23	Marne	FR	0.7200
FRE22	Oise	FR	0.7200
FRG01	Loire-Atlantique	FR	0.7200

FRC14	Yonne	FR	0.7200
FRC12	Nièvre	FR	0.7200
FRG02	Maine-et-Loire	FR	0.7200
FRB06	Loiret	FR	0.7200
FRB05	Loir-et-Cher	FR	0.7200
FRB04	Indre-et-Loire	FR	0.7200
FRB02	Eure-et-Loir	FR	0.7200
FRG03	Mayenne	FR	0.7200
FRG04	Sarthe	FR	0.7200
FR102	Seine-et-Marne	FR	0.7200
FRI34	Vienne	FR	0.7200
FRF24	Haute-Marne	FR	0.7200
FRE23	Somme	FR	0.7167

Table 4. Top 20 high fire risk RCP4.5 by NUTS3.

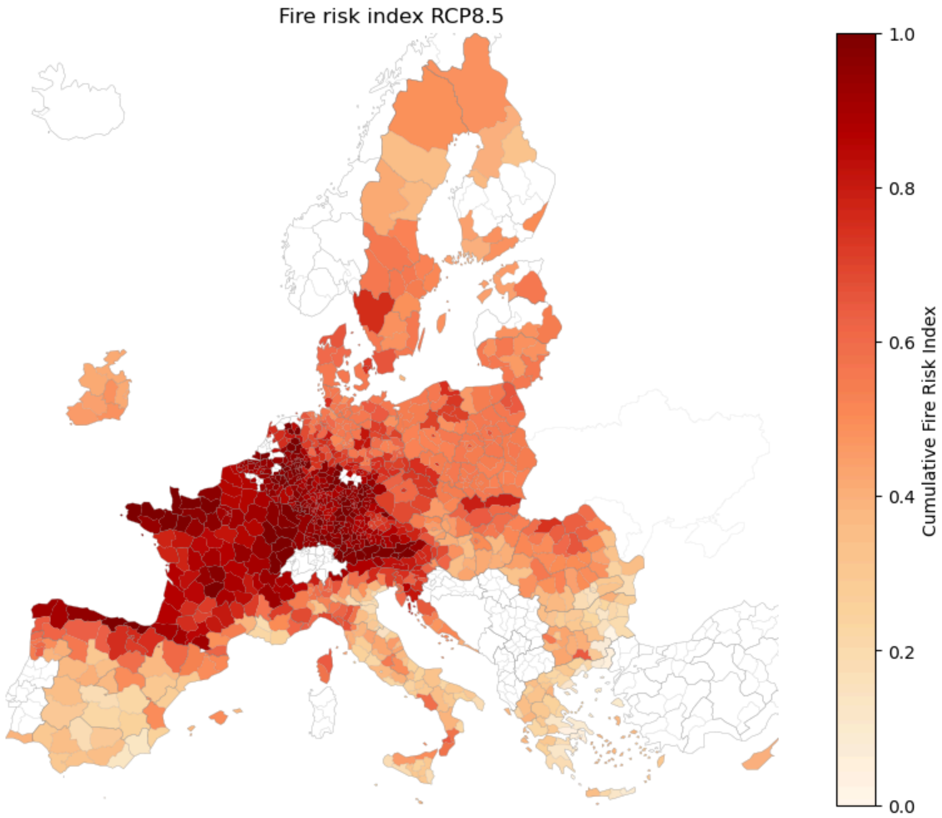

Figure 14. Unique fire risk RCP8.5.

NUTS_ID	NAME_LATN	CNTR_CODE	Fire_risk
FRG03	Mayenne	FR	1.0000
AT322	Pinzgau-Pongau	AT	1.0000

DEA14	Krefeld, Kreisfreie Stadt	DE	1.0000
FRD11	Calvados	FR	1.0000
FRD12	Manche	FR	1.0000
DE229	Regen	DE	1.0000
FRD21	Eure	FR	1.0000
AT226	Westliche Obersteiermark	AT	1.0000
DEA15	Mönchengladbach, Kreisfreie Stadt	DE	1.0000
DE251	Ansbach, Kreisfreie Stadt	DE	1.0000
DEA16	Mülheim an der Ruhr, Kreisfreie Stadt	DE	1.0000
AT222	Liezen	AT	1.0000
DEA17	Oberhausen, Kreisfreie Stadt	DE	1.0000
DE24B	Kulmbach	DE	1.0000
FRF24	Haute-Marne	FR	1.0000
DE27A	Lindau (Bodensee)	DE	1.0000
FRF33	Moselle	FR	1.0000
FRF34	Vosges	FR	1.0000
DE732	Fulda	DE	1.0000
DE27C	Unterallgäu	DE	1.0000

Table 5. Top 20 high fire risk RCP8.5 by NUTS3.

6.2 Heat waves risk

Evaluating the risk with the existent variables of the project has been used the following variables:

- Historical probability of heatwaves: maximum and mean
- Change in frequency of heatwaves: maximum and mean
- Time frame of heatwaves: mean
- Change in intensity of heatwaves: maximum and mean
- Time frame of heatwaves: maximum

All the previous variables are evaluated to be included in a unique risk assessment using the NUTS3 resolution. Figure 15, Figure 16 and Figure 17 show the cumulative fire risk on the different pathways. Thus, Table 6, Table 7 and Table 8 show the top 20 NUTS3 regions with high heat wave risk, where it can be observed that on RCP2.6, the risk is low in most of the areas, but on RCP4.5, the risk increases drastically on Spain, south of France, Italy, Sverige and with less risk on Ελλάδα. On RCP8.5, there is a high risk in all the countries. The column NUTS_ID is the identification on NUTS3, NAME_Latin is the region's name using the original naming, the CNTR_CODE is the country's designation, and the Fire risk is the normalized value of fire risk calculated.

Table VI shows that the regions with high risk are heterogeneous around countries, but there is a marked difference in the other scenarios. On the RCP 4.5 scenario, Table

VII shows that the south countries and Sverige are the most affected. And on the RCP8.5, Table VIII, the high risk is around all European countries.

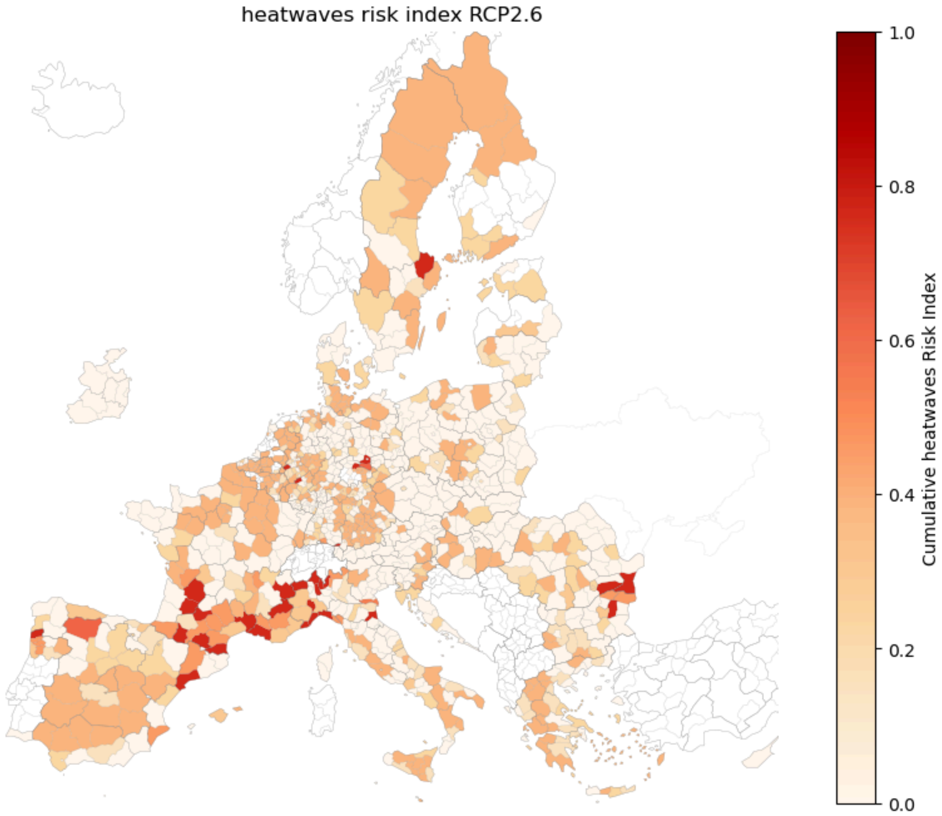

Figure 15. Unique heat wave risk RCP2.6.

NUTS_ID	NAME_LATN	CNTR_CODE	Heat wave risk
RO223	Constanţa	RO	0.7692
ITC33	Genova	IT	0.7692
ITC31	Imperia	IT	0.7692
DE27A	Lindau (Bodensee)	DE	0.7692
FRI11	Dordogne	FR	0.7692
DEA29	Heinsberg	DE	0.7692
PT111	Alto Minho	PT	0.7692
ITC14	Verbano-Cusio-Ossola	IT	0.7692
FRI14	Lot-et-Garonne	FR	0.7692
DEE0B	Saalekreis	DE	0.7692
DEG0D	Sömmerda	DE	0.7692
ITC17	Asti	IT	0.7692
FRJ12	Gard	FR	0.7692
ITC15	Novara	IT	0.7692

ITC41	Varese	IT	0.7692
SE121	Uppsala län	SE	0.7692
FRJ26	Hautes-Pyrénées	FR	0.7692
FRJ15	Pyrénées-Orientales	FR	0.7692
DEB12	Ahrweiler	DE	0.7692
ITC32	Savona	IT	0.7692

Table 6. Top 20 high heat wave risk RCP2.6 by NUTS3.

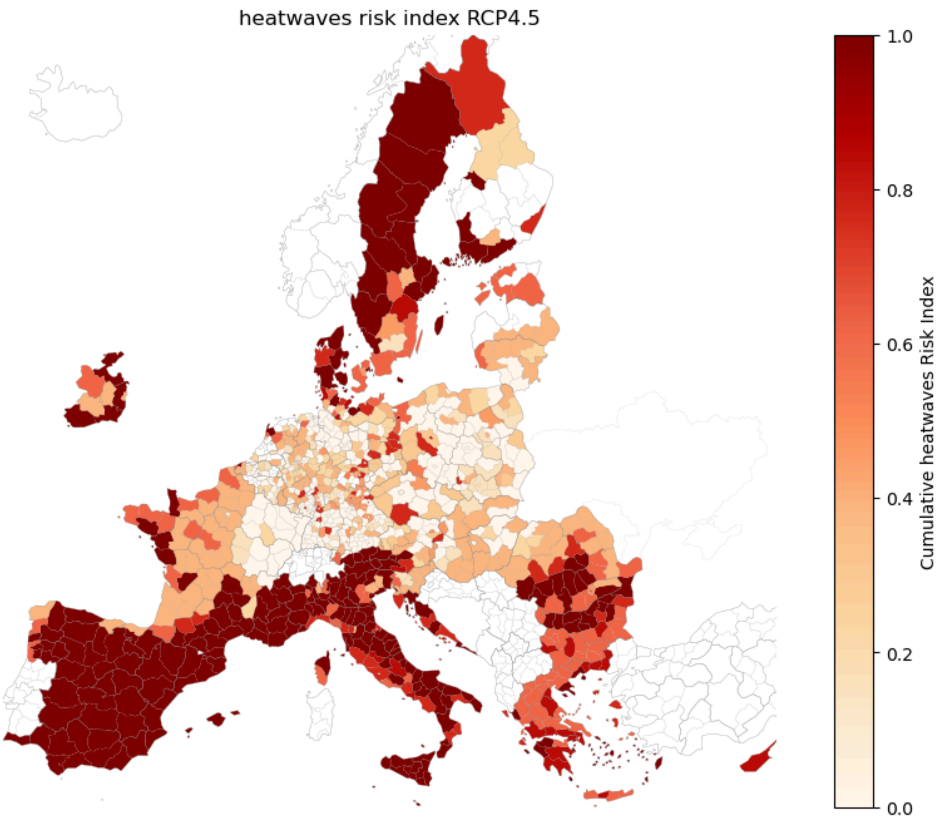

Figure 16. Unique heat waves risk RCP4.5.

NUTS_ID	NAME_LATN	CNTR_CODE	Heat wave risk
EL621	Zakynthos	EL	1.0000
FRH04	Morbihan	FR	1.0000
HR032	Ličko-senjska županija	HR	1.0000
HR031	Primorsko-goranska županija	HR	1.0000
FRJ26	Hautes-Pyrénées	FR	1.0000
FRJ23	Haute-Garonne	FR	1.0000
FRJ22	Aveyron	FR	1.0000
FRJ21	Ariège	FR	1.0000

NUTS_ID	NAME_LATN	CNTR_CODE	Heat wave risk
FRJ15	Pyrénées-Orientales	FR	1.0000
FRJ14	Lozère	FR	1.0000
FRJ13	Hérault	FR	1.0000
FRJ12	Gard	FR	1.0000
FRJ11	Aude	FR	1.0000
FRI31	Charente	FR	1.0000
FRG05	Vendée	FR	1.0000
HR037	Dubrovačko-neretvanska županija	HR	1.0000
EL421	Kalymnos, Karpathos, Kasos, Kos, Rodos	EL	1.0000
EL307	Peiraias, Nisoi	EL	1.0000
DK050	Nordjylland	DK	1.0000
DK042	Østjylland	DK	1.0000

Table 7. Top 20 high heat wave risk RCP4.5 by NUTS3.

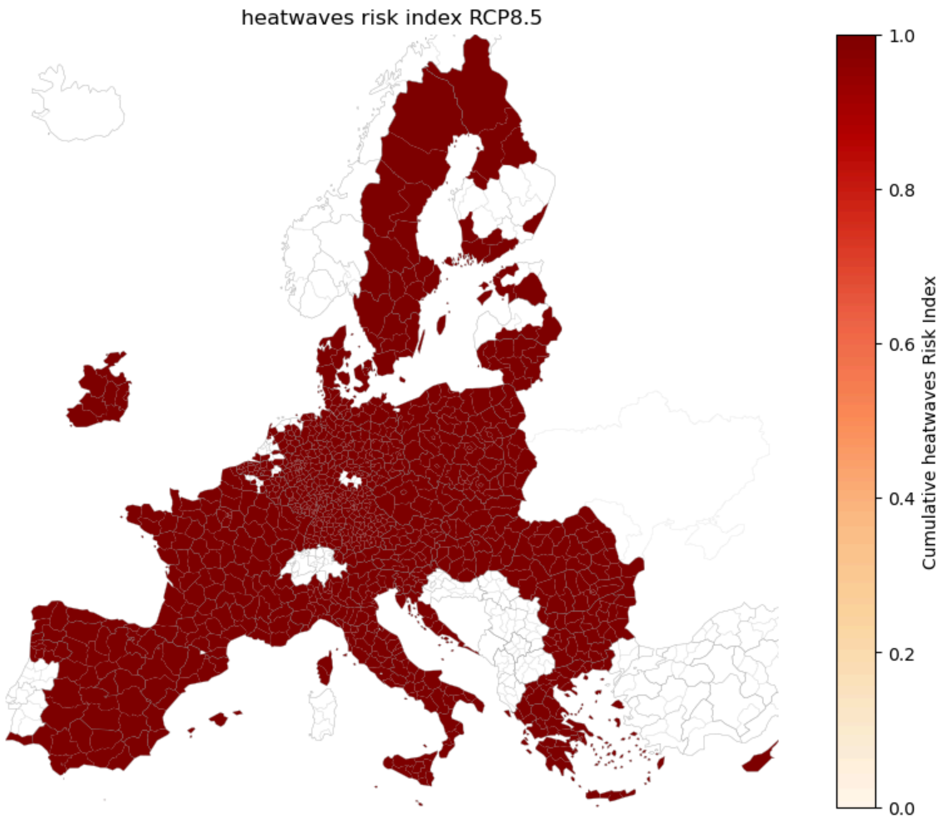

Figure 17. Unique heat waves risk RCP8.5.

NUTS_ID	NAME_LATN	CNTR_CODE	Heat wave risk
CY000	Kýpros	CY	1.0000
HU213	Veszprém	HU	1.0000
FRJ24	Gers	FR	1.0000
FRJ25	Lot	FR	1.0000
FRJ26	Hautes-Pyrénées	FR	1.0000
HR031	Primorsko-goranska županija	HR	1.0000
HR032	Ličko-senjska županija	HR	1.0000
HR033	Zadarska županija	HR	1.0000
HR034	Šibensko-kninska županija	HR	1.0000
HR035	Splitsko-dalmatinska županija	HR	1.0000
HR036	Istarska županija	HR	1.0000
HR037	Dubrovačko-neretvanska županija	HR	1.0000
HU110	Budapest	HU	1.0000
HU120	Pest	HU	1.0000
HU211	Fejér	HU	1.0000
HU212	Komárom-Esztergom	HU	1.0000
HU221	Győr-Moson-Sopron	HU	1.0000
FRJ22	Aveyron	FR	1.0000
HU222	Vas	HU	1.0000
HU223	Zala	HU	1.0000

Table 8. Top 20 high heat wave risk RCP8.5 by NUTS3.

7 Risk assessment due to the climate impacts in the energy sector

This section presents the results of Module 4.4, which assesses the impact on the energy system resulting from exposure to several index risks using the previously calculated RCP pathways. Additionally, a metric was used to define the effects: the percentage of aerial line kilometres affected by the country. This value can help to determine the impact on the zone or country by knowing the affected km versus all the line lengths.

The values shown in this section are not absolute indices but relative to the maximum risk overall in the scenarios. These indices are important but depend on the type of affectation, whether it affects a main electrical line or a small line, and the kind of maintenance of each region. More information would be needed to conclude details on the time fault resolution or other aspects related to the recovery. The following subsections explain the affectations of the different hazards.

7.1 Fire risk

The tool's results in terms of fire risk are displayed in the images in the following section. It first displays a general map view, showing the risk associated with the aerial lines and the percentage of kilometres of lines affected by country. The final section offers a closer examination of countries with relevant results to be explained in more detail.

Analysing the different RCP scenarios in Figure 18 shows the results in the RCP2.6; the risk in all zones is low, and therefore, there are no affected lines. There are some zones where the risk is higher but not enough to be a critical point.

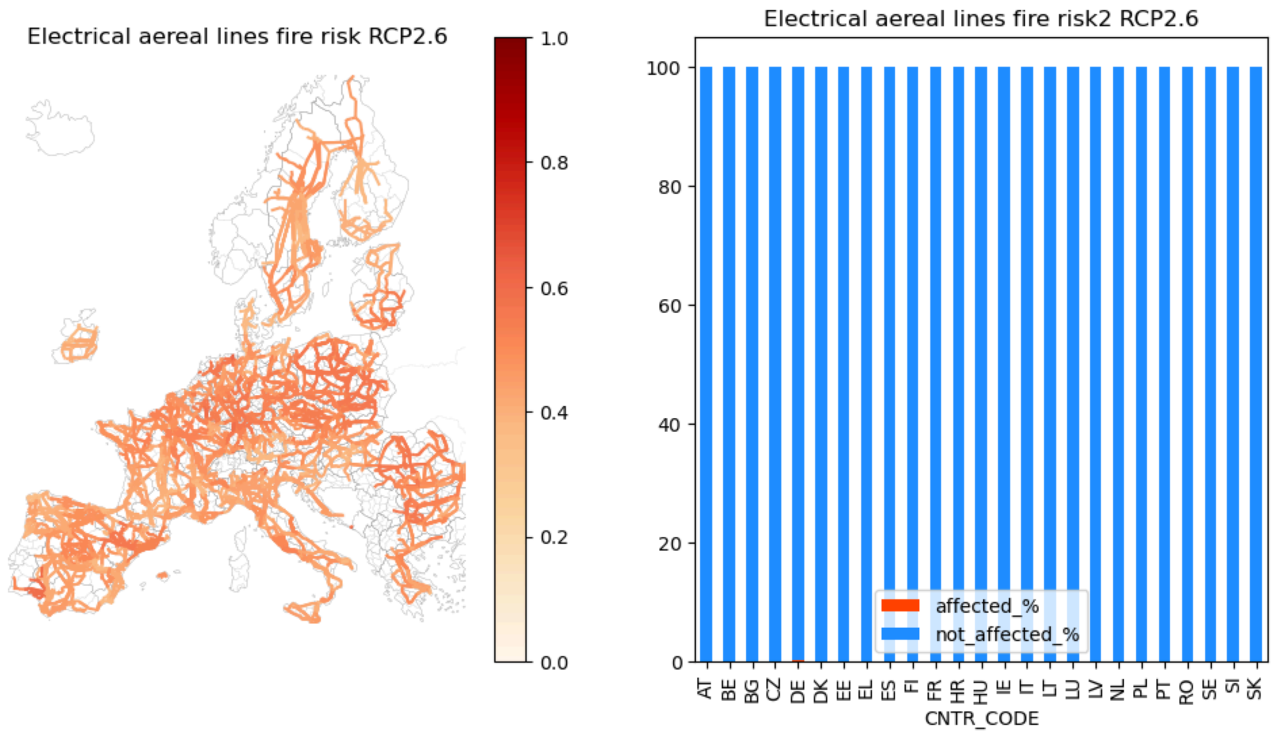

Figure 18. Aerial electrical lines risk (left) and percentage of km affected by country (right) on RCP2.6.

The figure 21 shows the results for the RCP4.5; the risk increases and specific regions in France and Belgium significantly contribute to this increase in the risk and affected lines. In Belgium, the risk grows up to 5% of the length of the electrical lines, but in France, the affected lines are more than 50%.

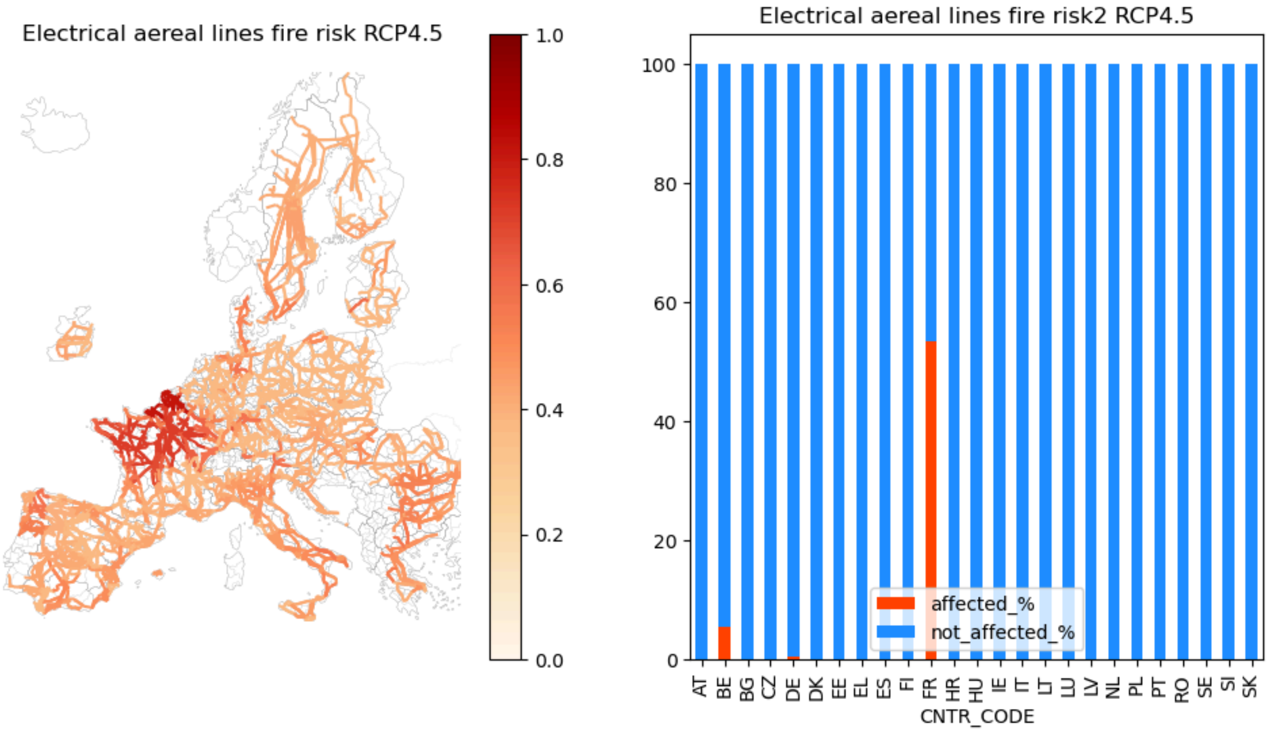

Figure 19. Aerial electrical lines risk (left) and percentage of km affected by country (right) on RCP4.5.

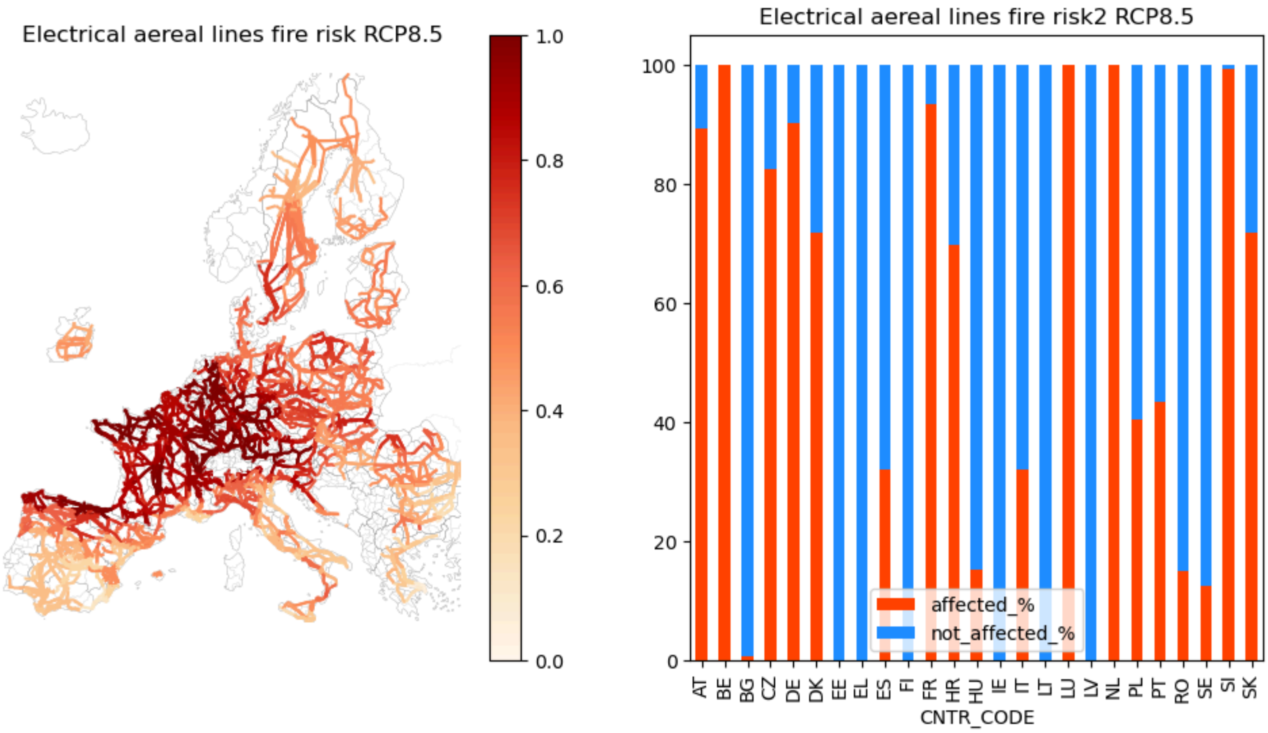

Figure 20. Aerial electrical lines risk (left) and percentage of km affected by country (right) on RCP8.5.

The figure shows the increase of risk in RCP8.5 cases. Now, the risk increases in most parts of European countries, especially Belgium, the Nederland, Slovenija and Luxembourg, where all the electrical lines are affected. More than 80% of the countries affected are Österreich, France, Deutschland and Česko. Most European countries are affected by this scenario in terms of fire risk. Table IX shows the percentage of kilometres affected by countries in the same scenario; 19 out of 25 countries evaluated have high-risk affectations on the energy sector by fire risk.

NAME_LATN	Affected lines %	Affected km	Total length km
Nederland	100.00	2208	2208
Luxembourg	100.00	276	276
Belgique/België	100.00	2357	2357
Slovenija	99.31	2097	2112
France	93.34	55323	59272
Deutschland	90.16	45107	50031
Österreich	89.27	6947	7782
Česko	82.61	7905	9569
Danmark	71.93	1094	1520
Slovensko	71.83	3037	4228
Hrvatska	69.68	1950	2798
Portugal	43.34	1656	3822
Polska	40.39	11671	28892
España	32.12	17767	55309
Italia	32.07	11214	34967
Magyarország	15.33	1145	7470
România	15.13	3146	20798
Sverige	12.63	3461	27397
Bulgaria	0.74	75	10201
Suomi/Finland	0.00	0	7441
Éire/Ireland	0.00	0	3913
Lietuva	0.00	0	3669
Elláda	0.00	0	7185
Latvija	0.00	0	929
Eesti	0.00	0	2253

Table 9. Aerial lines affected by fire risk on RCP8.5.

In conclusion to this hazard evaluation, the risk associated with the energy system, based on fire risk scenarios, is strongly dependent on the evolution of the RCP. In the RCP4.5 scenario, the impact of the energy sector is high in two countries, France and Belgium. However, in the worst-case scenario, the entire continent of Europe will face energy problems due to fire risks, thereby increasing the insecurity of the energy supply.

7.2 Heat waves risk

The images in the following section display the tool's results regarding heat wave risk. It first displays a general view of the map, showing the risk associated with the aerial lines and the percentage of kilometres of lines affected by country. The final section offers a closer examination of countries that have relevant results to be explained in more detail.

Analysing the different RCP scenarios in Figure 21 shows the results for the RCP2.6; the risk in all zones is low, but it can be observed that a few zones are affected. Bulgaria is the most affected country, with around 30% of the lines impacted, followed by Italy at 20%.

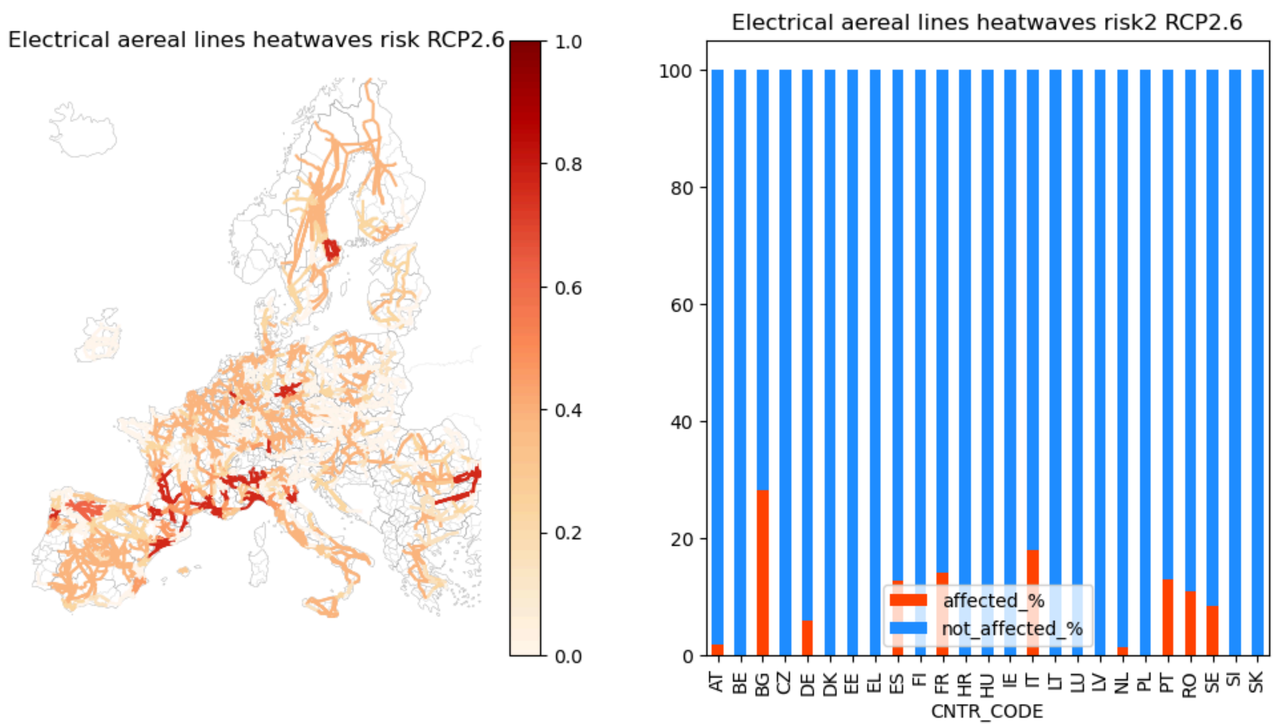

Figure 21. Aerial electrical lines risk (left) and percentage of km affected by country (right) on RCP2.6.

Figure 22 shows the results for the RCP4.5; the risk increases in specific regions in France and Belgium significantly contribute to this increase in the risk and affected lines. In Belgium, the risk grows up to 5% of the length of the electrical lines, but in France, the affected lines are more than 50%.

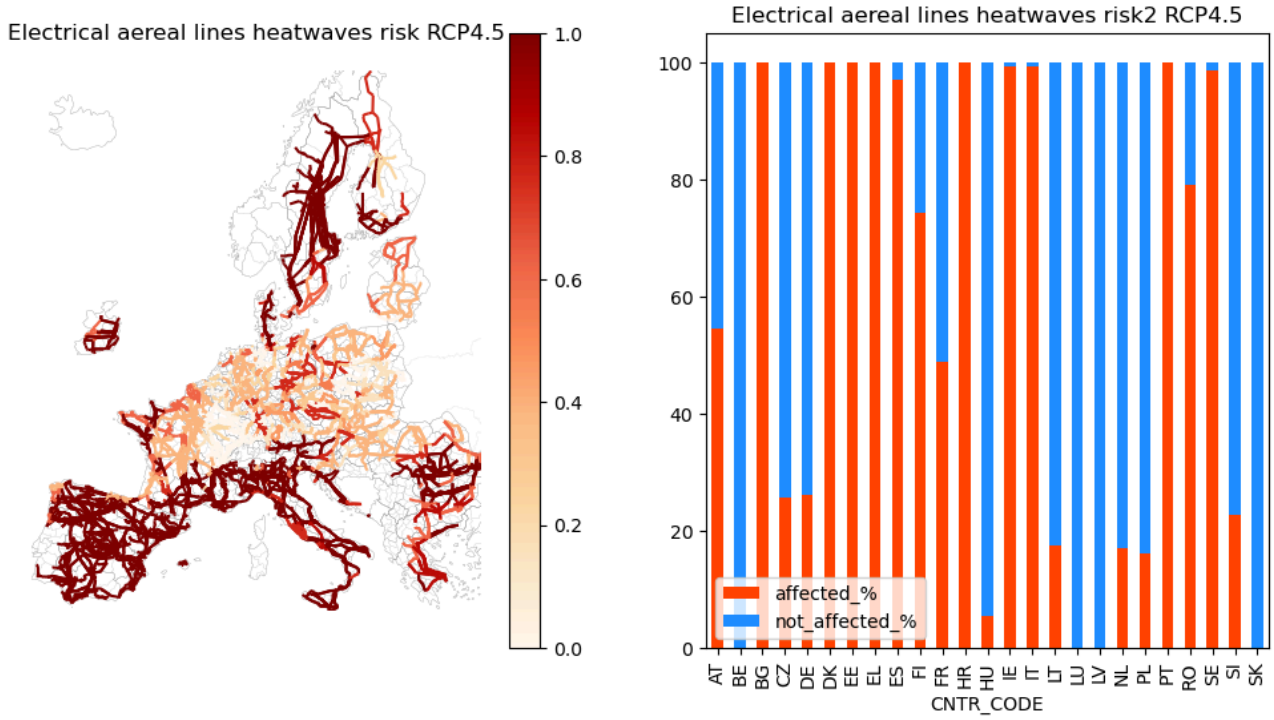

Figure 22 Aerial electrical lines risk (left) and percentage of km affected by country (right) on RCP4.5.

Figure 23 shows the results for the RCP4.5; the risk increases in almost all the countries. As shown in Table 10, only Latvija, Luxembourg, Belgium and Slovensko have no impact based on heat wave risk. Still, all the other countries are affected, and half of the evaluated countries have several implications on the energy systems. Something essential to explain is that the import of energy is not considered in this assessment because it is an indirect impact, and we cannot calculate this with the available information. For sure, if the countries that don't have high risk are energetically dependent on their neighbours and they are affected, then they will also be affected.

NAME_LATN	Affected lines %	Affected km	Total length km
Bulgaria	100.00	10201	10201
Danmark	100.00	1520	1520
Eesti	100.00	2253	2253
Elláda	100.00	7185	7185
Portugal	100.00	3822	3822
Hrvatska	100.00	2798	2798
Éire/Ireland	99.41	3890	3913
Italia	99.39	34753	34967
Sverige	98.73	27050	27397
España	97.03	53665	55309
România	79.12	16455	20798

NAME_LATN	Affected lines %	Affected km	Total length km
Suomi/Finland	74.26	5525	7441
Österreich	54.59	4248	7782
France	48.81	28929	59272
Deutschland	26.18	13097	50031
Česko	25.60	2450	9569
Slovenija	22.70	479	2112
Lietuva	17.55	644	3669
Nederland	17.09	377	2208
Polska	16.06	4641	28892
Magyarország	5.37	401	7470
Latvija	0.00	0	929
Luxembourg	0.00	0	276
Belgique/België	0.00	0	2357
Slovensko	0.00	0	4228

Table 10. Aerial lines affected by heat waves risk on RCP4.5.

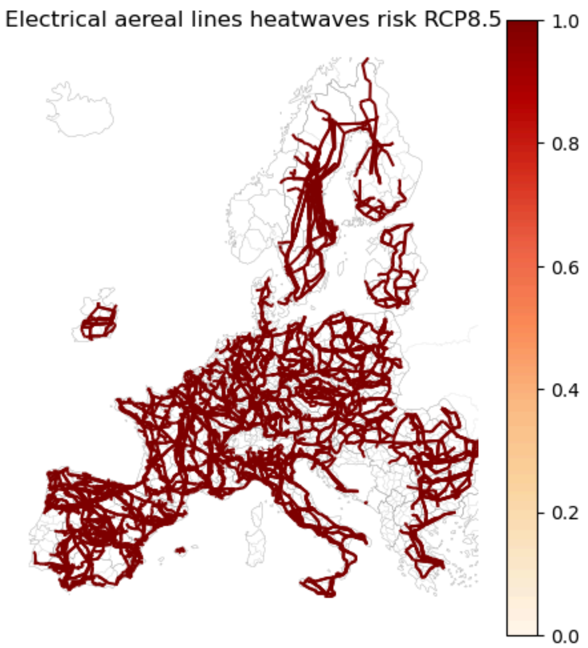

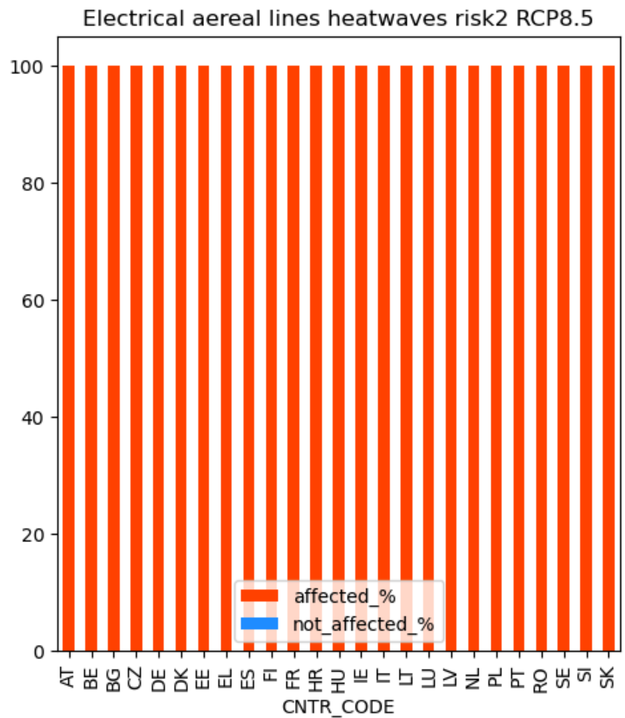

Figure 23. shows the increase of risk in RCP8.5 cases. Now, the risk increases in all parts of European countries, and there is no difference as all the electrical lines are affected by this risk, and the entire energy system evaluated would be affected by this risk.

In conclusion to this heat wave evaluation, the risk associated with the energy system, based on fire risk scenarios, strongly depends on the evolution of the RCP. In the RCP4.5 scenario, the energy sector's impact is high in half of the evaluated countries, and only five countries out of the 25 evaluated have no energy-related problems. However, in the worst-case scenario, the entire continent of Europe will face energy problems due to fire risks, thereby increasing the insecurity of the energy supply.

8 Conclusions

The deliverable presents a comprehensive analysis of climate change's impacts on the energy sector, with a particular focus on fire and heatwave risks across different regions. The document explains the calculation methods for floods, but similar calculations are used to obtain the indices for the other risks. It highlights how climate-related events can profoundly impact energy systems and infrastructure, underscoring the need for resilient and adaptive strategies to mitigate these risks.

Module 4.4 is introduced as a specialised tool designed for risk assessment in the energy sector. This module provides methodologies for evaluating climate impacts, including fire risks and heat waves, and offers frameworks for impact analysis correction and electrical model considerations. By addressing these challenges, Module 4.4 serves as an essential resource for understanding regional climate impacts and supporting decision-making processes in the energy sector.

The findings from Module 4.4 demonstrate that the energy sector will inevitably face significant challenges due to climate change, which will affect various regions in different ways based on the severity of these impacts. To enhance the resilience of energy systems, it is essential to prioritise expanding distributed energy resources and elevate the standards of control and assessment tools.

In summary, Deliverable 4.4 emphatically reinforces the critical importance of addressing climate-related risks in the energy sector and promotes Module 4.4 as an indispensable resource for strengthening resilience and effectively managing these risks with urgency and precision.

9 References

(n.d.). From http://www.enwl.co.uk/news-and-press/latest-news/2015/12/06/06-12-15-lancaster-and-surrounding-area-to-be-without-power-for-days-(06-00-update)

(n.d.). From http://www.enwl.co.uk/news-and-press/latest-news/2015/12/26/26-12-15-severe-flooding-causes-power-cuts-in-rochdale-and-lancashire-(12-20-update)

A. de Gross Domestic Product (GDP) in Barcelona . (n.d.). Barcelona, Barcelona,, España. Retrieved (accessed on Apr 8, 2020) from Available online: https://www.bcn.cat/estadistica/angles/dades/anuari/cap11/C1102010.htm .

Anderson, K., Li, X., Dalvi, S., Ericson, S., Barrows, C., Murphy, C., & Hotchkiss, E. (2020). Integrating the Value of Electricity Resilience in Energy Planning and Operations Decisions. IEEE Syst. J.

Barrientos, M., & Soria, C. (n.d.). Consumo de electricidad per cápita por país - Mapa Comparativo de Países. Retrieved (accessed on May 8, 2020) from - Mundo Available online: https://www.indexmundi.com/map/?v=81000&r=xx&l=es

Brown, T. H., & Schlachtberger, D. ((2018)). PyPSA: Python for Power System Analysis. *Journal of Open Research Software*, (1), 4. https://doi.org/10.5334/jors.188.

FEMA Multi-Hazard Loss Estimation Methodology. (n.d.). FEMA Multi-Hazard Loss Estimation Methodology, . In *Flood Model: Hazus-MH MR4 Technical Manual; 2009th ed.;* (p. 2009).

Grady, J. S. ((2019).). Emotions in storybooks: A comparison of storybooks that represent ethnic and racial groups in the United States. . *Psychology of Popular Media Culture,* , 8(3), 207–217. doi:https://doi.org/10.103

Herring, S., Hoerling, M., Peterson, T., & Stott, P. (2020,). Explaining extreme events of 2018 from a climate perspective. (pp. 95, S1–S96.). Bull. Am. Meteorol. Soc. .

INE Empresas por municipio y actividad principal. (n.d.). Retrieved (accessed on May 26, 2020). from Available online: https://www.ine.es/jaxiT3/Datos.htm?t=4721#!tabs-tabla,

JRC, E. (2019). The Future of Cities—Opportunities, Challenges and the Way Forward.

Karagiannis, G., Cardarilli, M., Turksezer, Z., Spinoni, J., Mentaschi, L., Feyen, L., & Krausmann, E. (2019;). *Climate change and critical infrastructure - storms.* ISBN 9789279964039.

Karagiannis, G., Turksezer, Z., Alfieri, L., Feyen, L., & Krausmann, E. (2017;). *Climate Change and Critical Infrastructure .* Floods ISBN 9789279754456.

Kawase, H., Imada, Y., Tsuguti, H., Nakaegawa, T., Seino, N., Murata, A., & Takayabu, I. (2020). *The heavy rain event of July 2018 in Japan enhanced by historical warming.* Bull. Am. Meteorol. Soc. .

Kelsey Jordahl, J. V. (2020). geopandas/geopandas: v0.8.1 (v0.8.1). Zenodo . doi:https://doi.org/10.5281/zenodo.3946761

Koks, E., Pant, R., Thacker, S., & Hall, J. (2019,). Understanding Business Disruption and Economic Losses Due to Electricity Failures and Flooding. Int. J. . Disaster Risk Sci.

L. Grigsby, L. (2018;). *The Electric Power Engineering Handbook; 3rd Editio.; .* ISBN 9781315222363.

M.D.C.Y.T. DE GUÍA TÉCNICA DE APLICACIÓN DEL REGLAMENTO ELECTROTÉCNICO PARA BAJA TENSIÓN. (2003). ESPAÑA,.

Mahoney, K. (2020). *Extreme hail storms and climate change: Foretelling the future in tiny, turbulent crystal balls?* Bull. Am. Meteorol. Soc.

Monjo, R., Paradinas, C., Gaitán, E., Redolat, D., Prado, C., Pórtoles, J., . . . al., e. (2019). *Report on extreme weather events prediction - deliverable D1.3.*

Murphy, C., Hotchkiss, E., Anderson, K., Barrows, C., Cohen, S., Dalvi, S., . . . al., e. (2020). Adapting Existing Energy Planning, Simulation, and Operational Models for Resilience Analysis.

O'Donohue, W. ((2017).). Content analysis of undergraduate psychology textbooks (ICPSR 21600; ICPSR., Version V1) [Data set]. doi: https://doi.org/10.3886/ICPSR36966.v1

Ouellette, J. .. ((2019, November 15)). Physicists capture first footage of quantum knots unraveling in superfluid. . (A. Technica., Ed.) From https://arstechnica.com/science/2019/11/study-you-can-tie-a-quantum-knot-in-a-superfluid-but-it-will-soon-untie-itself

Pant, R., Thacker, S., Hall, J., Alderson, D., & Barr, S. (2018). Critical infrastructure impact assessment due to flood exposure. . J. Flood Risk Manag.

Panteli, M., & Mancarella, P. (2015). Modeling and Evaluating the Resilience of Critical Electrical Power Infrastructure to Extreme Weather Events. *IEEE Systems Journal, PP*, 1-10. doi:10.1109/JSYST.2015.2389272

Poljanšek, K., Bono, F., & Gutiérrez, E. .. (2010;). *GIS-Based Method to Assess Seismic Vulnerability of Interconnected Infrastructure A Case of EU Gas and Electricity Networks;* (ISBN 9789279152092 ed.).

Redolat, D., Monjo, R., Paradinas, C., Pórtoles, J., Gaitán, E., Prado-Lopez, C., & Ribalaygua, J. (2020,). Local decadal prediction according to statistical/dynamical approaches. Int. J. Climatol.

Resilience to Flooding of Grid and Primary Substations. ETR 138 ANNEX Issue 1 2018. (2018.).

Russo, B., Velasco, M., Monjo, R., Martínez-Gomariz, E., Sánchez, D., Domínguez, J., . . . Gonzalez, A. (2020,). Evaluación de la resiliencia de los servicios urbanos frente a episodios de inundación en Barcelona. In *El Proyecto RESCCUE. Ing. del agua* (p. 24).

Sánchez-Muñoz, D., Domínguez-García, J., Martinez-Gomariz, E., Russo, B., Stevens, J., & Pardo, M. (2020,). Electrical grid risk assessment against flooding in Barcelona and Bristol cities. . Sustain.

Statista Urbanization, b. c. (2019 , (accessed on May 2020). 28). *Statista*. From Available online: https://www.statista.com/statistics/270860/urbanization-by-continent/

United Nations Transforming our world: The 2030 agenda for sustainabledevelopment. (2016).

Vasenev, A., Montoya, L., & Ceccarelli, A. (2016). A hazus-based method for assessing robustness of electricity supply to critical smart grid consumers during flood events. . Proc. - 2016 11th Int. Conf. Availability, Reliab. Secur. ARES 2016.

Winter, J., Huang, H., Osterberg, E., & Mankin, J. (2020). *Anthropogenic impacts on the exceptional precipitation of 2018 in the mid-Atlantic United States.* Bull. Am. Meteorol. Soc.